along the nitrogen cycle determining sources of $NO_3^-$is difficult. The presence of fecal coliform jointly with NO_3^- in groundwater may indicate recent NO_3^- contamination by human sewage or animal droppings provided this is confirmed by another reliable technique [1]. Stable nitrogen isotope techniques enable the identification of sources based on the characteristic or distinctive nitrogen isotope compositions and are valuable tools for the detection of the origin. Different sources of stable isotope characteristic values are not affected by changes in concentrations within water; therefore, the isotope forms of NO_3^- in water are relatively stable [18].

Dual isotope analysis of nitrate ($\delta^{15}N$-NO_3^- and $\delta^{18}O$-NO_3^-) has been frequently used to differentiate NO_3^- sources because of the distinct isotopic characteristics of themain NO_3^- sources, such as rain, chemical fertilizers, and NO_3^- derived from nitrification [19, 20]. Sacchi *et al*.[21] used the isotopes to trace the nitrate-N in the groundwater of the central Po plains in Italy and they discovered that in the higher plains, groundwater pollution mainly originated from four sources: (1) a high osmotic pressure aquifer in the vadose zone of the region; (2) a higher underground water level; (3) an intensive cattle industry that produces a large amount of fecal matter; and (4) a large amount of irrigation water. Kelley*et al*. [20] used nitrogen and oxygen isotope ratios to identify nitrate sources and dominant nitrogen cycle processes in a tile-drained dryland agricultural field. Liu *et al*. [22] tracked sources of groundwater nitrate contamination using nitrogen-oxygen dual isotopes around Beijing, China. Nitrogen-oxygen dual isotope analysis has been established as a tool in providing important information regarding the origin of nitrate contamination in groundwater, the contribution of different sources to a multi-source plume, and the rate and mechanisms of the contamination, as well as in evaluating the success of contaminated site remediation. Zhang *et al*. [23] used the ^{15}N isotope to analyze groundwater nitrate pollution and sources in Beijing's Fangshan district, and the results suggested that NO_3^--N in groundwater mainly originated from animal waste, wastewater, and organic soil nitrogen. Westover *et al*.[24]investigated water quality and sources and processes influencing NO_3^- in the Kettle River basin using a combination of chemical and isotopic techniques. Based on $\delta^{15}N$ values and concentration data, NO_3^-in surface waters originates primarily from natural soil nitrification processes, with additional influences from anthropogenic activities, such as waste water effluents at sampling locations downstream from population centres.

This study aims to define the NO_3^--N sources and understand the contamination of groundwater in Hebei plain (HP) and provide a scientific basis for controlling NO_3^--N pollution in the groundwater of HP and utilization of groundwater. We first investigated data from 21 wells in the shallow groundwater of HP, evaluated the NO_3^--N pollution concentrations in the groundwater, compared the NO_3^--N pollution concentrations of groundwater in different areas, and traced the sources of NO_3^--N.

STUDY SITE

Hebei Plain is south of Beijing and Tianjin, and spans to Bohai in the east and abuts the Taihang Mountains in the west. The study region is situated between a latitude 36°03' to 40°02' and a longitude 114°15' to 119°50', and is one of the alluvial fan plain zones(Figure 1). The area has a continental, semi-arid climate with a mean annual temperature of 12-13ºC, and summer maximum and winter minimum of 45.8 and -28.2 ºC, respectively and with annual precipitation of 400-800 mm. The precipitation is dominated by the Asia summer monsoon during July and August, which accounts for about 70% of the annual precipitation. There is usually only 40-60 mm of rainfall, or even no rainfall, for more than 100 days in spring. The variation of seasonal precipitation is so large that it is the common case to have dry spring and flooding summer. Mean potential evaporation ranges from 1,100 to 1,800 mm. Based on landforms, HP can be divided into three areas: the piedmont area, the central area, and the coastal area [25, 26].

The HP accessible groundwater mainly occurred in the Quarternary sediment aquifers. The regional Quaternary aquifers consist of fluvial fans, alluvial fans and lacustrine deposits [27]. Vertical distribution of the aquifer has been described in detail. A thick sedimentary sequence has been deposited in the HP, with a depth of 500-600 m in depressions, 350-450 m in uplift areas, and 150-300 m around the alluvial fan. From the top to the bottom, sediments can be divided into four aquifer groups according to the lithologic properties, geological age, the distribution of aquifers and aquicludes, and hydrodynamic conditions (Figure 1) [28].

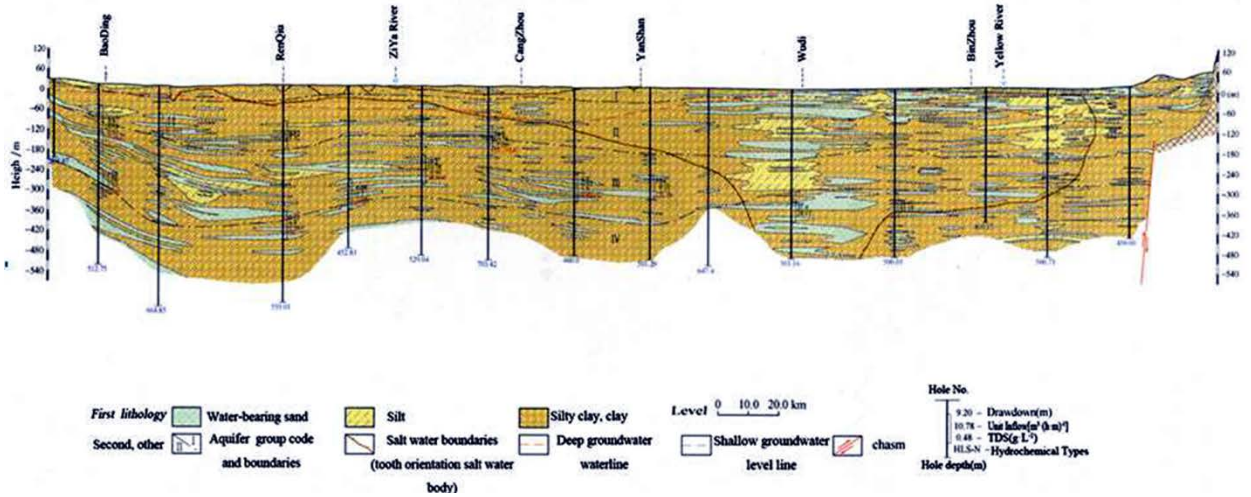

Fig.1. Baoding-Cangzhou hydrogeologic profile in Hebei Plain

The depth of the first aquifer group (shallow unconfined aquifer) ranged between 10 and 50 m, with coarse-grained sand in the piedmont area to fine-grained sand in the littoral plain. The second aquifer group was a series of shallow semi-confined aquifers with buried depths of 120-210 m, with sandy gravel, medium to fine sand. The second group was the major aquifer for groundwater exploitation for agricultural irrigation. The third aquifer group, underlying the second aquifer group, had lower boundary between 170 and 3 350 m. This formation consists of sandy gravel in the piedmont area and medium to fine sand in the central and littoral plain.

The fourth aquifer group lays below 350 m with a thickness of 50-60 m, which consists of cemented sandy gravel and thin layers of weathered sand [29].According to groundwater exploitation and aquifer distribution, groundwater can be divided into shallow groundwater mainly occurring in the first aquifer group (shallow aquifers), while deep groundwater occurs in the latter three groups (deep aquifers).

EXPERIMENTAL

Groudwater sampling and analytical methods

Groundwater samples, including 21 wells of the National hydrological monitoring network, were collected from three areas of Hebei plain in May and September from 2009 to 2015, representing 10.09 % of the Monitoring network in HP. The well depths of the quaternary groundwater ranged from 4.5 to 50 m. Eight samples (numbers 1-8) were taken from the piedmont area of Shijiazhuang, six samples (numbers 9-14) were taken from the central area ofHengshui and seven samples (numbers 15-21) were taken from the coastal area of Cangzhou(Figure2). Water samples were collected from active pumping wells used either for domestic or agricultural purposes, and were initially preserved in a cold box and later transferred to a refrigerator in the laboratory. Samples were filtered with 0.45μm membrane filters for measurement of ion concentrations and isotopic compositions. The concentrations of major cations and anions were measured by inductively coupled plasma-optical emission spectrometry (ICP-OES) and ion chromatography(IC), respectively. Ion charge imbalances were within ±5%.

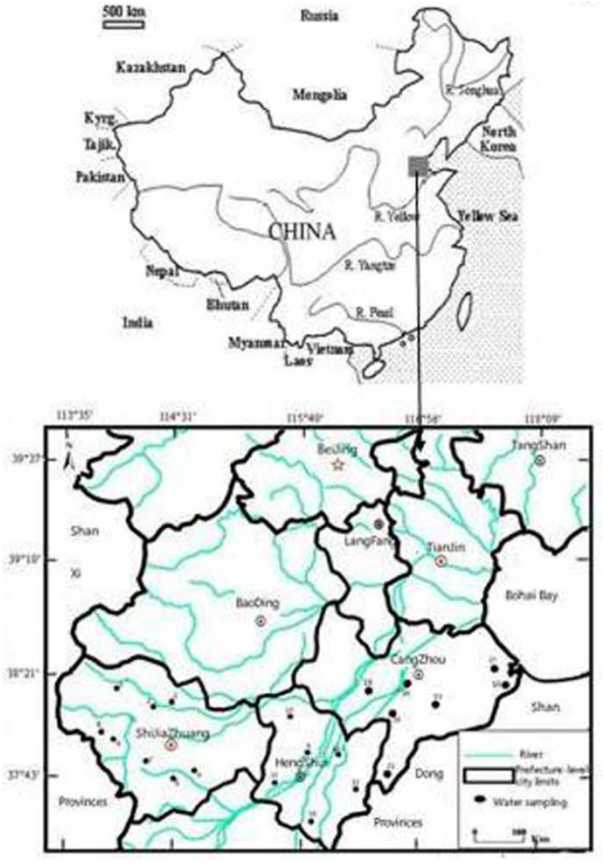

Fig. 2. Location of the shallow groundwater sampling sites in the study area.

Eight samples (numbers 1-8) were collected from Shijiazhuang to represent the Piedmont Plain. Six samples (numbers 9-14) were collected from Hengshui to represent the Central Plain. Seven samples (numbers 15-21) were collected from Cangzhou to represent the Eastern Coastal Plain.

Stable isotope ratios were reported in parts per thousand (‰) using the conventional delta notation: $\delta_{sample}=[(R_{sample}-R_{standard})/R_{standard}]\times1000‰$, where R represents the $^{18}O/^{16}O$, or $^{2}H/^{1}H$ ratios of the samples and standards, respectively. $\delta^{18}O_{H2O}$ and δDwere determined at the Key Laboratory of Groundwater Sciences and Engineering, Ministry of Land and Resources, Chinese Academy of Geological Sciences (CAGS), using online thermal conversion elemental analysis isotope ratio mass spectrometry (TC/EA-IRMS). The precision of measurements was ±0.1‰ and ±1‰, respectively, and results were reported relative to V-SMOW. In the field, 3-5 L samples were collected to ensure 60—80 mg of nitrate on the cation exchange resin. After removing SO_4^{2-} by addition of $BaCl_2$ to 300 mL of water, the water was passed through the cation exchange resin and became acidity, with a flow rate of 2-5 mL·min^{-1} by adjusting the stopcock on the separatory funnel. The KNO_3 and KCl solutions were produced by adding 1 mol·L^{-1} KOH solution eluent to neutral, and were dried at 90ºC. $\delta^{15}N_{NO3}$ and $\delta^{18}O_{NO3}$ were determined at the same time in one sample input using online high-temperature pyrolysis of 500 μg KNO_3. N_2 and CO generated by KNO_3 and C reaction were separated through a chromatographic column at 60ºC coupled with ConFloIV and IRMS, and the precision of $\delta^{15}N$ and $\delta^{18}O$ was 0.25‰ and 0.6‰, respectively, compared with that of 0.1‰ and 0.5‰ abroad. All experiments were performed in duplicate and thedata were populated in Excel and plotted with Origin 9.0.

RESULTS

Chemical concentrations of groundwater

The chemical and isotopic compositions of the groundwater are listed in Table1 and Figure3, respectively. Chemical elements of shallow groundwater were analyzed to derive the statistical analysis of anion and cation concentrations in the study areas. The average cation concentrations in Shijiazhuang ranked as follows: $Ca^{2+}>Na^{+}>Mg^{2+}>K^{+}$; anion concentrations ranked as follows: $HCO_3^{-}>SO_4^{2-}>Cl^{-}>NO_3^{-}>CO_3^{2-}$. The average cation concentrations in Hengshui ranked as follows: $Na^{+}>Mg^{2+}>Ca^{2+}>K^{+}$; anion concentrations ranked as follows: $SO_4^{2-}>HCO_3^{-}>Cl^{-}>NO_3^{-}>CO_3^{2-}$. The average cation concentrations in Cangzhou ranked as follows: $Na^{+}>Ca^{2+}>Mg^{2+}>K^{+}$; anion concentrations ranked as follows: $Cl^{-}>HCO_3^{-}>SO_4^{2-}>NO_3^{-}>CO_3^{2-}$. Both Table 1 and Fig. 3 show that the sum of SO_4^{2-} and Cl^{-} averagely accounted for between 40% and 60% of total anions in the piedmont area, around 70% in the central area, and 90% in the coastal area. Besides, the sum of Ca^{2+} and Mg^{2+} averagely accounted for 80% of total cations in the piedmont area, 50% in the central area, and 40% in the coastal area.

The order of the average of the anion concentrations was $HCO_3^{-}>SO_4^{2-}>Cl^{-}>NO_3^{-}>CO_3^{2-}$; greater than 25 Meq% were HCO_3^{-} and SO_4^{2-}, and that of the cation concentrations was $Ca^{2+}>Na^{+}>Mg^{2+}>K^{+}$ in the piedmont area. The order of the average of the anion concentrations was $SO_4^{2-}>HCO_3^{-}>Cl^{-}>NO_3^{-}>CO_3^{2-}$; greater than 25 Meq% were Cl^{-}, SO_4^{2-}, and that of the cation concentrations was $Na^{+}>Mg^{2+}>Ca^{2+}>K^{+}$ in the central area. The order of the average of the anion concentrations was $Cl^{-}>HCO_3^{-}>SO_4^{2-}>NO_3^{-}>CO_3^{2-}$; greater than 25 Meq% were Cl^{-}, and that of the cation concentrations was $Na^{+}>Ca^{2+}>Mg^{2+}>K^{+}$ in the coastal area. According to Shoka Lev's classification method, the main hydrochemical types from the piedmont area, the central area to the coastal area changed from HCO_3-Ca·Mg, through HCO_3·SO_4-Na·Ca and SO_4·Cl-Na·Ca, to SO_4·Cl-Na.

Table1. Results for hydrochemistry and isotopes in shallow groundwater, a-rural, town; b-farmland.

Sampling Point	Depth (m)	NO_3^{-} (mg·L^{-1})	Cl^{-} (mg·L^{-1})	SO_4^{2-} (mg·L^{-1})	$\delta^{15}N$ (‰)	$\delta^{18}O$ (‰)	$\delta^{2}H$ (‰)	$\delta^{18}O$ (‰)
1. Sanhepu[a]	15.0	17.95	23.60	105.21	2.62	-3.36	-54	-8.7
2. Hantai[a]	30.0	14.49	41.23	112.92	5.08	-5.47	-62	-8.4
3. Licun[b]	30.0	15.14	54.46	144.76	8.43	-4.86	-57	-7.6
4. Ciyu[a]	17.0	15.21	44.97	118.20	—	—	-61	-8.2
5. Shanyincun[b]	12.0	17.73	56.75	165.95	13.31	-1.31	-60	-8.4
6.Luquanchengguan[a]	16.2	16.99	54.52	178.95	8.78	-4.14	-62	-8.4
7. Yongbi[a]	34.0	10.76	109.21	123.75	10.7	-3.95	-63	-8.6
8. Luquanshiqu[a]	30.0	17.95	205.03	145.37	8.24	-5.24	-63	-8.7
9. Balizhuang[a]	10.0	2.34	547.58	596.75	—	—	-61	-7.6
10. Nanjili[b]	13.0	1.56	167.81	210.24	—	—	-64	-8.7
11. Zhangquan[b]	20.0	5.47	1448.25	562.73	18	6.64	-56	-7.3
12. Wanglou[b]	38.0	6.28	377.02	359.47	11.96	-1.53	-62	-8.5
13.Donganzhuang[b]	36.0	4.73	565.67	902.91	13.04	-1.78	-59	-7.8
14. Xiaoying[b]	29.0	2.89	1857.80	1457.49	—	—	-58	-7.9
15. Mengcun[b]	30.0	9.72	1088.23	531.72	14.06	4.34	-62	-8.4
16. Xiasanbao[a]	4.5	61.14	514.16	390.79	18.06	-4.86	-57	-7.9
17.Yangerzhuang[a]	5.8	78.64	773.71	346.83	20.46	-2.13	-65	-8.9
18. Hechengjie[b]	50.0	16.05	323.10	412.01	—	—	-63	-8.7
19. Jiaohe[b]	12.0	7.61	521.68	507.95	17.09	0.77	-69	-9.2
20. West of Cangzhou[a]	12.0	9.78	578.64	494.47	30.99	9.94	-50	-6.4
21. Xinji[a]	6.2	23.48	1728.98	487.00	—	—	-51	-6.4

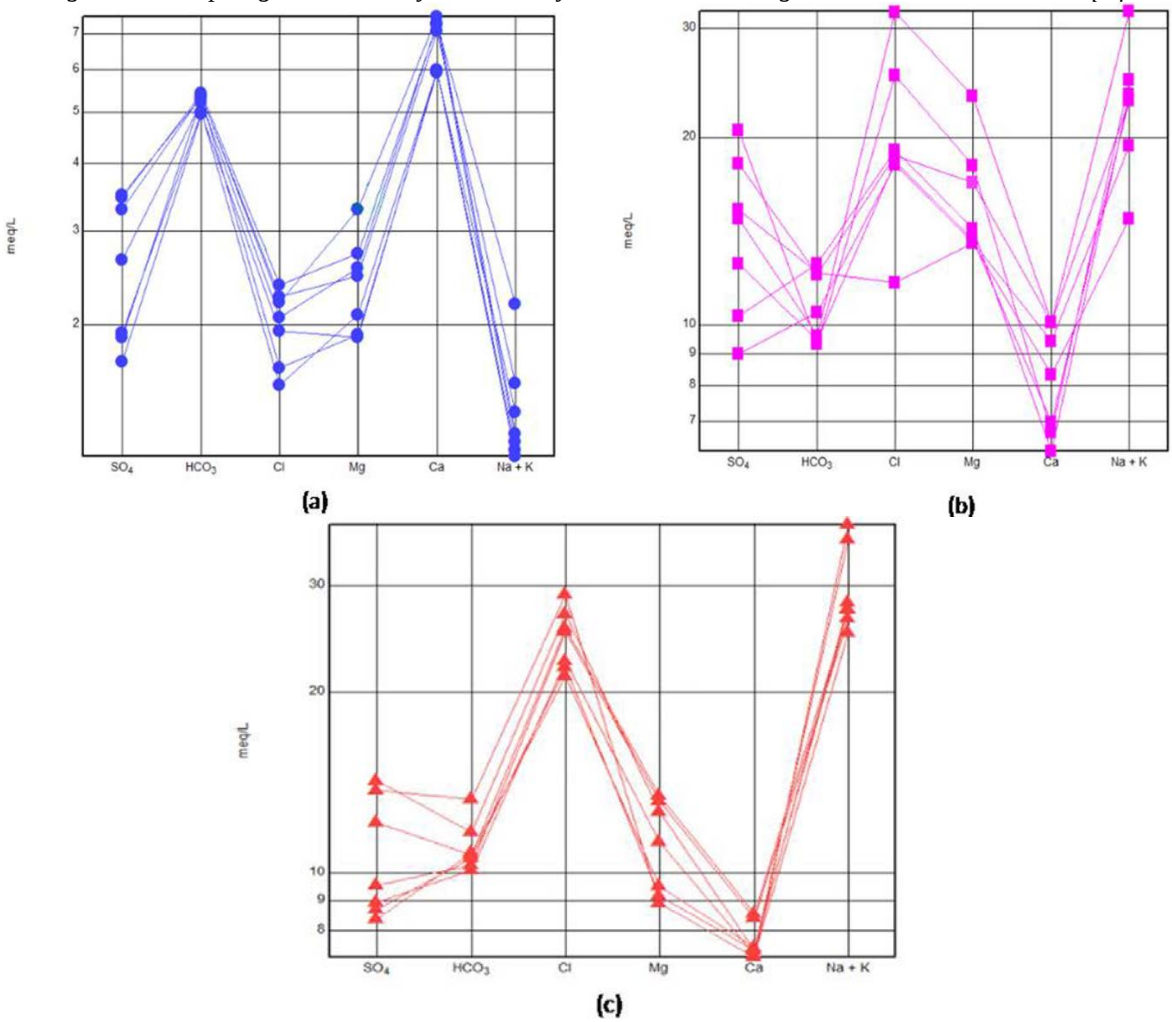

Fig.3. Hydrochemical composition of Shijiazhuang(a) , Hengshui(b) and Cangzhou(c).

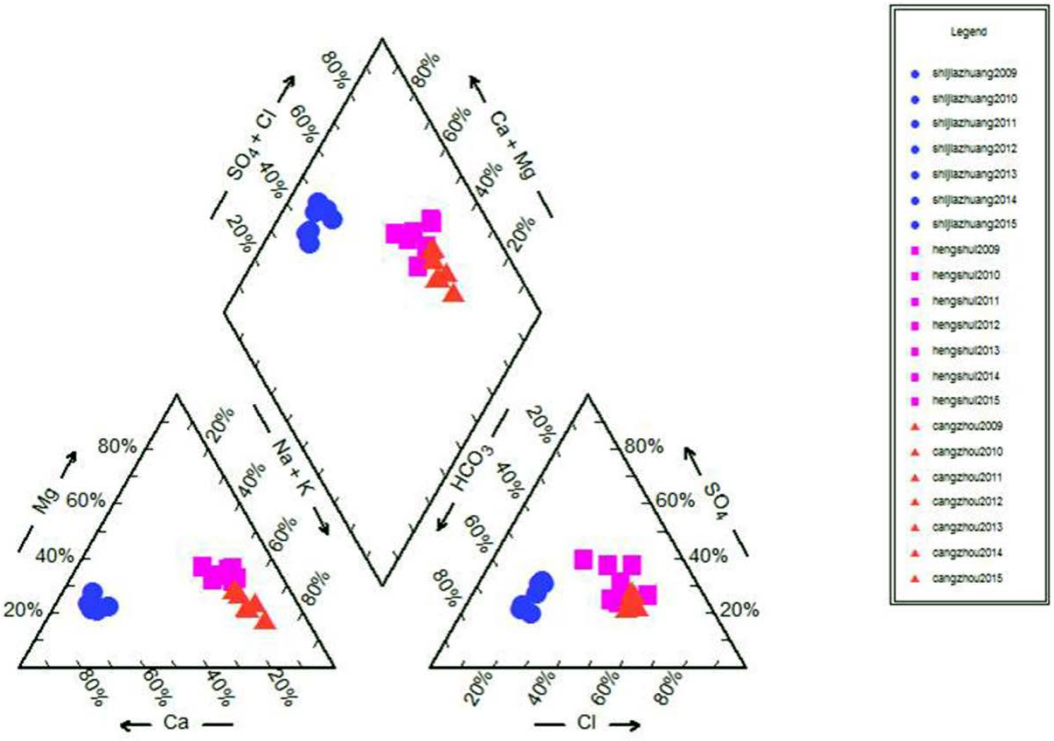

Fig.4. Piper figure of water chemistry of Shijiazhuang, Hengshui and Cangzhou.

As seen from Piper diagram of water chemistry(Figure 4), anion and cation distribution was again more scattered from the piedmont area to the coastal area, and the hydrochemical type changed from bicarbonate-type to sulfate-chloride type and chloride-type, and salinity gradually increased.It confirmed that in the piedmont area and the central area, the chloride-type area decreased, while the bicarbonate-type and sulfate-chloride type areas increased, as shallow groundwater constantly gained riverside-leakage and recharged from water sources and precipitation. The coastal area experienced larger salinity due to seawater intrusion, in addition to evaporation.

In the Piedmont Plain and the Central Plain, the chloride-type area was small, while the bicarbonate-type and sulfate-chloride type areas were larger, as shallow groundwater constantly gained riverside-leakage and recharged from water sources and precipitation. The Eastern Coastal Plain experienced larger salinity due to seawater intrusion, in addition to evaporation.

Isotope compositions ofwater

Table1 and Figure 5 illustrate the 21 stable deuterium and oxygen isotopes determining results of the shallow groundwater samples. In the piedmont area, δ2H and δ18O values ranged from -63‰ to -54‰, and -8.7‰ to -7.6‰, respectively, and mean values were -60.25‰ and -8.38‰, respectively. In the central area, δ2H and δ18O values ranged from -64‰ to -56‰, and -8.7‰ to -7.3‰, respectively, and mean values were -60‰ and -7.97‰, respectively. In the coastal area, δ2H and δ18O values ranged from -69‰ to -50‰, and -9.2‰ to -6.4‰, respectively, mean values were -59.57‰ and -7.99‰, respectively. Based on the comparison, the δ2H and δ18O values of groundwater in the piedmont area are relatively small while the values in the central area are relatively large.

Because most of the world's precipitation is derived from evaporation of seawater, the δ2H and δ18O compositions of precipitation throughout the world are linearly correlated. In Figure 5, all data were close to the LMWL(δ2H=7.02341 δ18O+1.72339, R2=0.95) [23], and shifted to the right of the global meteoric water line(GMWL) [30]. It suggests that groundwater was mainly derived from local meteoric water. Most of samples were enriched in δ18O isotope and were located to the right of the LMWL, which indicates that the meteoric water experienced different extents of evaporation before the precipitation recharged. From the relationship shown in Figure 5, the linear relationship is approximately parallel to the RMWL, showing that aquifer of the study area has been recharged by precipitation.

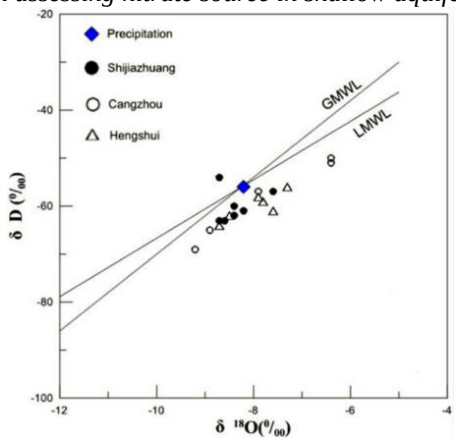

Fig.5. Plots of δ^2H and $\delta^{18}O$ in groundwater of Hebei Plain.Legend of lines: GMWL line indicates global meteoric water line; LMWL line indicates North China Plain's meteoric water line.

DISCUSSION

Distribution of nitrate-N

The range of NO_3^--N concentrations was 1.56-78.64 mg·L^{-1}in shallow groundwater of HP. The lowest level was collected in Balizhuang in the central area, and the highest level was in Yang'erzhuang in the coastal area. The mean concentration of NO_3^--N was 15.78 mg·L^{-1} in the piedmont area, 3.88 mg·L^{-1} in the central area, and 29.49 mg·L^{-1}, the largest concentration, in the coastal area.

Figure 6 illustrates the trends of NO_3^--N and chloride in HP. Chloride ranged from 27.98 to 2086.75 mg·L^{-1}, with a mean value of 518.16 mg·L^{-1}; NO_3^--N ranged from 3.08 to 92.59 mg·L^{-1}, with a mean value of 17.96 mg·L^{-1}; and sulfate ranged from 57.04 to 1324.21 mg·L^{-1}, with a mean value of 416.78 mg·L^{-1}. The lowest concentrations of NO_3^--N were in the central area, the largest changes in NO_3^--N concentrations were in the coastal area, and the lowest concentrations of chloride were in the piedmont area.

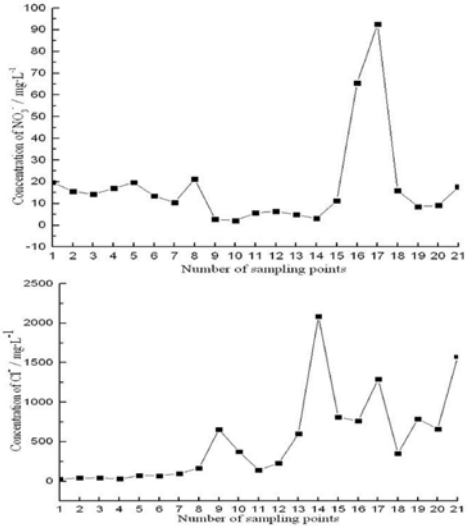

Fig.6. Contents of chloride and nitrate ions atthe sample points of the study area.

Table2. NO_3^--N content from 2009 to 2015

Year	Nitrate – N ranges	Average of May ±standard error ($mg \cdot L^{-1}$)	Average of September ±standard error ($mg \cdot L^{-1}$)	Annual averages	10$mg \cdot L^{-1}$ Exceeding factor (%)
2009	0.00~108.45	16.09±6.22	16.33±6.10	16.21	33.33
2010	0.00~87.30	18.74±4.57	15.66±4.43	17.20	54.76
2011	0.00~102.74	17.51±5.31	17.24±5.23	17.37	52.38
2012	0.00~121.50	21.97±5.92	21.29±5.78	21.63	59.52
2013	0.30~103.00	20.74±4.91	21.63±5.04	21.18	71.43
2014	0.44~58.53	18.09±3.63	13.32±3.27	15.70	46.34
2015	0.00~56.20	16.22±3.62	12.08±2.46	14.15	50.00

Average concentrations of chloride and nitrate at the Piedmont Plain, the Central Plain, and the Eastern Coastal Plainsampling points are along the abscissa and the content of the sampling points along the vertical axis.

The mean concentrations of chloride in the piedmont area, the central area, and the coastal area were 73.72, 827.36, and 789.79 $mg \cdot L^{-1}$, respectively. SO_4^{2-}/Cl^- ratios were 1.86, 0.82, and 0.57, respectively, and SO_4^{2-}/Cl^- ratios of the three areas were quite different. This significant variation indicates that the chloride and sulfate in the groundwater have different sources. Unlike SO_4^{2-}/Cl^-, NO_3^-/Cl^- ratios differed slightly between the three areas. The NO_3^-/Cl^- ratio of the piedmont area ranged from 0.09 to 0.76, with a mean value of 0.32; the central area ratio ranged from 0.00 to 0.12, with a mean value of 0.01; and the coastal area ratio ranged from 0.01 to 0.12, with a mean value of 0.05. The narrow range of the NO_3^-/Cl^- ratios suggests that the input of NO_3^--N and chloride reached a steady state [31].

General chardcteristics of nitrate

Table2 shows the overall state of NO_3^--N in groundwater of HP from 2009 to 2015. An obvious upward trend in NO_3^--N levels appeared. The NO_3^--N concentrations escalated from 16.21 $mg \cdot L^{-1}$ in 2009 to 21.18 $mg \cdot L^{-1}$ in 2013. However, NO_3^--N concentrations differed between sampling sites; areas of low concentration were mainly located in Nanjili and Xiaoying in the central area, and areas of high concentration were mainly in Yang'erzhuang and Xiasanbao in the coastal area.According to the SDWQC (10 $mg \cdot L^{-1}$), the concentrations of NO_3^--N in groundwater of HP from 2009 to 2015 exceeded the standard. Analyzing the NO_3^--N in samples determined a large range of NO_3^--N concentrations in groundwater of HP was found, 0.00-121.50 $mg \cdot L^{-1}$, and the mean value was 17.64 $mg \cdot L^{-1}$ during the seven-year monitoring period, exceeding the SDWQC (10 $mg \cdot L^{-1}$)by a factor of 1.76.

According to Muller's established groundwater geochemistry background value of 2.0 $mg \cdot L^{-1}$ of NO_3^--N [32], the influence of human activity on NO_3^--N concentrations in groundwater had increased.

The maximum concentration occurred between 2009 and 2010, rising from 33.33% to 54.76%, an increase of 21.43%. There were 25 valuesexceeding 10 $mg \cdot L^{-1}$, accounting for 59.52% of all samples in 2012; 30 values exceeding 10 $mg \cdot L^{-1}$, accounting for 71.43% of all values in 2013; and the values exceeding the SDWQC reached 46.34% in 2014, and 50.00% in 2015. Nitrate concentration was higher in May than in September except in 2009 and 2013 due to heavier rainfall in July and August, it may have resulted from relatively abundant rainfall, and enhanced the link between a saturated zone and an unsaturated zone [33].The soil of unsaturated zone exhibits strong adsorption of ammonia-nitrogen. Ammonia-nitrogen was prone to nitrification by oxidation in alkaline groundwater, resulting in nitrate, nitrite, and nitrate-nitrogen produced by nitrite due to its instability, thus increasing NO_3^--N concentrations in groundwater [34].

Regional changes of nitrate-N

Figure 7 shows the trend of NO_3^--N concentrations in the three main sub-plains of HP from 2009 to 2015. Changing concentrations of NO_3^--N are evident in three areas, while the coastal area had the highest concentrations of NO_3^--N, followed by the piedmont area, and then the central area, which was the lowest one, although it, too, showed an increasing trend.

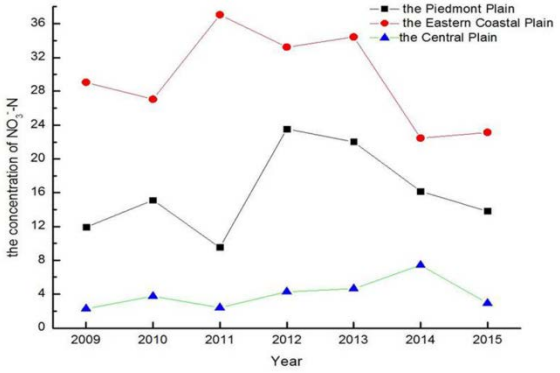

Fig.7. Variation of shallow groundwater nitrate-N concentration in sub-plain of Hebei plain.

Trend of NO_3^--N concentrations in the three main sub-plains of Hebei Plain from 2009 to 2015.

There were evident changes in NO_3^--N concentrations in each sub-plain, with the highest concentrations of NO_3^--N recorded in the Eastern Coastal Plain, followed by the Piedmont Plain and the Central Plain, which, while lowest, still exhibited an increasing trend.

The coastal area, with the highest NO_3^--N concentrations, had an annual mean value of 29.49 $mg \cdot L^{-1}$, exceeding the SDWQC (10 $mg \cdot L^{-1}$) by a factor of 2.95. The value of NO_3^--N in this area remained greater than 25 $mg \cdot L^{-1}$ during the study period, with peak value reached in May 2012 about 37.42 $mg \cdot L^{-1}$, exceeding the SDWQC by a factor of 3.74. The lowest value was 19.41 $mg \cdot L^{-1}$ in September 2014, exceeding the standard by a factor of 1.95. The high NO_3^--N concentrations in the coastal area from 2009 to 2015 may be related to manure and waste emissions, as well as the structure and composition of the unsaturated zone, which greatly influences the infiltration of pollutants, resulting in contamination of shallow groundwater.

The mean concentration of NO_3^--N in the piedmont area was 15.78 $mg \cdot L^{-1}$, exceeding SDWQC by a factor of 1.58. The minimum level, 9.71 $mg \cdot L^{-1}$, was recorded in May 2011, and the next lowest level, 9.34 $mg \cdot L^{-1}$, was recorded in September 2011; hence, the measurements taken in 2011 were the only two during the study period in this area that did not exceed the SDWQC. The maximum concentration, 23.71 $mg \cdot L^{-1}$, was recorded in May 2012, which could have resulted from the larger solids of that vadose zone. The wider the granules in a vadose zone, the stronger permeability it offered, and thus easier nitrification. Due to this characteristic, coupled with an accumulation of NO_3^--N from excessive fertilization carried through rainfall or irrigation, NO_3^--N leached through the vadose zone to shallow groundwater, resulting in a generally higher nitrate concentration in the area.

The mean concentration of NO_3^--N in the central area was 3.88 $mg \cdot L^{-1}$. It was, therefore, the least polluted of the three areas. Low concentration mainly result because the central area had fine rock particles in the unsaturated zone, and more clay interlayer [35], which are conducive to denitrification. Still, NO_3^--N concentrations in this area demonstrated a rising trend overall. The minimum value occurred in May 2009, 1.67 $mg \cdot L^{-1}$, and the highest concentration was recorded in May 2014, 11.34 $mg \cdot L^{-1}$. From 2009 to 2013, the NO_3^--N concentration levels did not exceed the SDWQC. However, the 2014 levels exceeded the standard by a factor of 1.13, which may have resulted from the topography of the central area. Within this area, sources of pooling along the groundwater flow coming water after entering the contaminated area, which increases its NO_3^--N concentration.

Sources of NO_3^--N

The $\delta^{15}N$ and $\delta^{18}O$ results of the shallow groundwater are shown in Table1. In the three areas, nitrogen and oxygen isotopes demonstrated significant changes. In the piedmont area, $\delta^{15}N$ and $\delta^{18}O$ values ranged from 2.62‰ to 13.31‰, from -5.47‰ to -1.31‰, respectively, with mean values of 8.17‰ and -4.05‰, respectively. Changes of nitrogen and oxygen isotope values of the central area were small compared to the piedmont area. $\delta^{15}N$ and $\delta^{18}O$ values ranged from 11.96‰ to 18.00‰, from -1.78‰ to 6.64‰, respectively, with mean values of 14.33‰ and 1.11‰, respectively. Oxygen and nitrogen isotopes of the coastal area showed the greatest changes in the three areas. $\delta^{15}N$ and $\delta^{18}O$ values ranged from 14.06‰ to 30.99‰, from -4.86‰ to 9.94‰, respectively, with mean values of 20.13‰ and 1.61‰, respectively.

Different values of $\delta^{15}N$ can be used to determine different sources of NO_3^--N in water. Generally, we can use $\delta^{15}N$ as a tracer of NO_3^- sources; however, there is an overlapping phenomenon in some sources of $\delta^{15}N$, such as sewage and manure. Therefore, in this study, $\delta^{18}O$ was combined with $\delta^{15}N$ to determine nitrate contamination.

Research byFenech *et al*. [30]indicated that $\delta^{15}N$ compositions of most terrestrial material fall between -10‰ to +25‰, and, as a result, isotope values of N and O can be useful in identifying the origin of groundwater NO_3^-. The $\delta^{15}N$ from atmospheric nitrogen deposition is about 0‰ to +13‰ and from manure about +5‰ to +25‰. Fertilizers generally have $\delta^{15}N$ values between 0‰ ± 4‰, and organic soil N is characterized by $\delta^{15}N$ values between 4‰ and 9‰. The $\delta^{18}O$ from atmospheric deposition isfrom +25‰ to +70%. The $\delta^{18}O$ values of atmospheric precipitation range between +20‰ to +70‰. Generally, synthetic fertilizers have $\delta^{18}O$ values between 22‰ ± 3% [36]

Figure 8 shows the sources of NO_3^--N in HP. The main sources of NO_3^--N in shallow groundwater were from manure and waste. NO_3^--N contamination in the piedmont area came from fertilizers, whereas NH_4^+ came from rainfall and soil nitrogen. The main forms of agriculture crop consisted of wheat and corn in which no manure was applied. Additionally, atmospheric-N deposition and soil nitrogen cannot significantly elevate the NO_3^--N concentrations. Therefore, it was demonstrated that fertilizers were a major source of NO_3^--N. Contamination of NO_3^--N in the central area and the coastal area was mainly derived from manureand waste.Sources of NO_3^--N of the Piedmont Plain originated mostly from fertilizers, while NO_3^--N of the Central Plain and the Eastern Coastal Plain was mainly derived from septic tank waste.

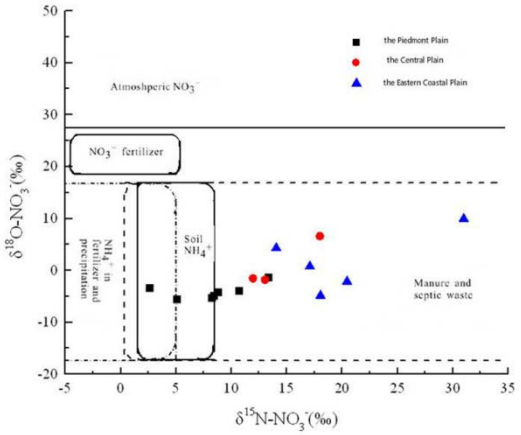

Fig.8. Sources of NO_3^--N in shallow groundwater of the study area.

CONCLUSIONS

(1) In the study area, the average chloride concentration was 527.73 mg·L^{-1}; the NO_3^--N mean concentrations were 16.95 mg·L^{-1}; and the sulfate mean concentrations were 397.88 mg·L^{-1}.The SO_4^{2-}/Cl^- ratios of the three areas differed significantly and NO_3^-/Cl^- ratios were only slightly different, indicating that chloride, NO_3^--N, and sulfate in groundwater had different sources.

(2) From 2009 to 2015, the NO_3^--N concentrations in groundwater ranged from 0.00-121.5 mg·L^{-1}, and the mean values was 17.64 mg·L^{-1}, exceeding the SDWQC by a factor of 1.76. Different areas had different concentrations of NO_3^--N.

The coastal area displayed the highest concentration, 29.49 mg·L^{-1}, which exceeds the SDWQC by a factor of 2.95. The piedmont area maximum concentration was 15.78 mg·L^{-1}, exceeding by a factor of 1.58. The concentration of NO_3^--N in the central area was the lowest one, averaging 3.88 mg·L^{-1}, and did not exceed SDWQC.

(3) Hydrochemical types in the study area displayed obvious differences. The hydrochemical type changes from bicarbonate-type to sulfate-chloride type and then to chloride-type, as shallow groundwater in the areas follows a migration pattern from the piedmont area to the coastal area and salinity gradually increased. The coastal area, with the largest salt content, experiences seawater intrusion. Groundwater was of meteoric origin, and a large proportion was subject to evaporation. In the area, the aquifer system was recharged from irrigation return flow and seawater intrusion.

(4) The isotope analysis of $\delta^{15}N$ and $\delta^{18}O$ in shallow groundwater of the three areas indicated that the NO_3^--N was mainly due to manure and waste, NH_4^+- to fertilizers. NO_3^--N of the coastal area and the central area was mainly due to manure and waste; and NH_4^+- mainly to fertilizers in the piedmont area.

Acknowledgments: *This work was supported by the National Natural Science Foundation of China (No. 41373096) and the Key Laboratory of Biological for Containment Prevention in Hebei, China. We thank engineers Chenxi Xing, ZhenjunTian, and Jianyou Qin from Hebei Hydrology and Water Resources Survey Bureau for assisting in the field survey.*

REFERENCES

1. 1. H.Amiri, M. Zare, D. Widory,*Isot. Environ. Healt. S.*, **51** (3), 392 (2015).
2. 2.I.Matiatos,*Sci. Total Environ.*, **541**, 802(2016).
3. 3.K.M.Rogers, E. Nicolini, V. Gauthier,*J. Contam. Hydrol.*, **138-139**, 93(2012).
4. 4.E.Elisante,A.N.N. Muzuka,*Environ. Earth Sci.*, **75**(3), 277(2016).
5. 5.Z.X.Chen,L. Yu, W.G. Liu, MHW Lam,G.J. Liu, N Ornelas-Soto,*Environ. Earth Sci.*,**71**(1), 217(2014).
6. 6.A.E.Lawniczak, J. Zbierska, B. Nowak, K. Achtenberg, A. Grzeskowiak, K.Kanas, *Environ.Monit. Assess.*,**188**(3),172(2016).
7. 7.C.Tamez-Meléndez, A. Hernández-Antonio, P.C. Gaona-Zanella,N. Ornelas-Soto,J. Mahlknecht, *Environ.Earth Sci.*,**75**(9),1(2016).
8. 8.L.Xing, H. Guo, and Y. Zhan, *J. Asian Earth Sci.*, **70–71**(1),250(2013).
9. 9.J.Zhi, A. Ding, S. Zhang, *Desalin. Water Treat.*, **57**(18),8243(2016).
10. 10.J.-j.Fang,A.-g. Zhou, C.-m. Ma, C.-f. Liu, H.-s Cai,Y.-q. Gan, Y.-d. Liu,*J. Cent.South Univ.*, **22** (2), 610 (2015).
11. 11.E.Minet, C.E. Coxon, R. Goodhue,K.G. Richards,R.M. Kalin, W. Meier-Augenstein,*Water Res.*, 46 (12),3723 (2012).
12. 12.P.Saccon, A. Leis, A. Marca, J. Kaiser, L. Campisi, M.E. Böttcher, J.Savarino, P. Escher, A.Eisenhauere, J.Erbland, *Appl. Geochem.*, **34** (4),75 (2013).
13. 13.A.R.Albertin, J.O. Sickman, A. Pinowska, R.J. Stevenson, *Biogeochemistry*, **108** (1),219 (2012).
14. 14.S.L.Li, C.Q. Liu, J. Li, Z. Xue, J. Guan, Y. Lang, H.Ding, L.Li, *Environ. Earth Sci.*,**68** (1)219 (2013).
15. 15.G.Michalski, M. Kolanowski, K.M. Riha, *Isot. Environ.HealtS.*,**51**(3),382(2015).
16. 16.F.J.Yue,C.Q. Liu, S.L. Li, Z.Q. Zhao, X.L.Liu, H. Ding, B.J. Liu, J.Zhong, *J. Hydrol.*,**519**,329 (2014).
17. 17.W.Wang, X. Song, Y. Ma, *Environ.Earth Sci.*,**75**(11),1(2016).
18. 18.S.K.Wexler, K.M. Hiscock, P.F. Dennis, *J. Hydrol.*,**468–469**, 85(2012).
19. 19.A.Nestler,M. Berglund, F. Accoe, S. Duta, D. Xue, P. Boeckx, P. Taylar, *Environ. Sci. and Pollut. R.*, **18** (4), 519 (2011).
20. 20.C.J.Kelley, C.K. Keller, R.D. Evans, C.H.Orr, J. L.Smith, B. A.Harlow, *Soil Biol. Biochem.*,**57** (3),731 (2013).
21. 21.E.Sacchi, M. Acutis, M. Bartoli, S. Brenna, C.A. Delconte, A. Laini, M. Pennisi,*Appl. Geochem.*, **34**(4), 164 (2013).

22. 22.M.Liu, A.S.M. Seyf-Laye, T. Ibrahim, D.B. Gbandi, H. Chen,*Environ. Earth Sci.*, **72** (3),707 (2014).
23. 23.X.Y.Zhang, B.D. Xin, W.C. Liu, Y.Q. Ji, X.H. Wang, W. Zhao,*Safety & Environ. Engin.*,**12** (3),15 (2011).
24. 24.M.D.Westover, L.K. Hall, C.C. Day, R.N. Knight, R.T. Larsen, Brock R. McMillan, *Annual Meeting of the American Society of Mammalogistsat Portland, Oregon*,2011.
25. 25.X.D. Li, *Water Sciences & Engineering Technology*, **236**(7),21(2013).
26. 26.F.Zhang, F. Shi, X. Li, X.Jia. *Int. Conference on Bioinformatics and Biomedical Engin.*, 2010.
27. 27.X.Lu, M. Jin, M.T.V. Genuchten, B.Wang, *Groundwater*,**49** (2), 286 (2011).
28. 28.Q.Sun, R. Kröbel, T. Müller, V. Römheld, Z.Cui, F.Zhang, X.Chen, *Agr. Water Manage.*, **98** (5),808 (2011).
29. 29.Z.W.Xu, X.Y. Zhang, G.R. Yu, X.M. Sun, X.F. Wen, *Environ. Sci.*,**35** (8),3230 (2014).
30. 30.C.Fenech,L. Rock, K. Nolan, J. Tobin, A. Morrissey, *Water Res.*, **46** (7), 2023(2012).
31. 31.Y.Uchida, T. Ishii, Y. Taguchi, *Bull.Geological Survey Japan*,**60**(1/2),87(2009).
32. 32.O.Rahmati, A.M. Melesse, *Sci.Total Environ.*, **568**,1110(2016).
33. 33.X.N.Zhou, S.Y. Liu, Z. Wang, Z.C. Zhou, *Water Sci. Engin. Technol.*, **2**,15(2008).
34. 34.J.Pei, H. Yao, H. Wang, J. Ren, X. Yu, *Water Res.*, **99**, 122 (2016).
35. 35.J.M.Thomas, A.H. Welch, M.D. Dettinger, *Psychopathology*, **37**(6),285(1996).
36. 36.Q.Yi, Y. Gao, H. Zhang, H. Zhang, Y.Zhang, M. Yang,*Chem. Engin. J.*, **300**, 139 (2016).

ИЗОТОПНА ИДЕНТИФИКАЦИЯ И ХИДРОХИМИЯ КАТО ИНСТРУМЕНТИ ЗА ОЦЕНКА НА ИЗТОЧНИЦИТЕ НА НИТРАТИ В ПЛИТКИЯ ВОДОНОСЕН ХОРИЗОНТ НА РАВНИНАТА ХЕБЕЙ, КИТАЙ

Х. Панг[1],Дж. Фанг[2], И. Лиу[1],Х.Цаи[3],Ф. Лиу[4], Т. Гао[1*]

[1]Училище по наука за околната среда и инженерство и лаборатория по биологична технология за предотвратяване на аварии в провинция Хебей, Хебейски университет по наука и технология, Шиджиажуанг, 050018, Китай

[2]Департамент по инженерна геология, Професионален колеж по земни ресурси на Хебей, Ухан 430090, Китай
[3]Училище по околната среда и лаборатория по биогеология и геология на околната среда, Университет по геонауки,Ухан 430074, Китай

[4]Институт по хидрогеология и геология на околната среда, CAGS, Шиджиажуанг, 050061,Китай

Постъпила на 18 фдекември 2017, приета на 31 януари 2018

(Резюме)

Равнината Хебей играе важна роля в Китай, където градските, земеделските и промишлените води силно зависят от подпочвените водни ресурси. За устойчиво използване на подпочвените водни ресурси е необходимо да се изследват хидрохимичните характеристики на плитката водоносна зона. Основните компоненти на подпочвените води свидетелстват за ясно зониране от предпланинската област през централната област до крайбрежната област, като хидрохимичният тип се променя от HCO_3-SO_4-Ca-MgиHCO$_3$-Cl-Ca-MgtypesдоHCO$_3$-SO_4-Na-Ca, SO_4-Cl-Na-CaиSO$_4$-Cl-Na. Проведено е изследване с помощта на деутерий и стабилни изотопи на кислорода за изясняване на потоците от подпочвени води. Подпочвените води имат валежен произход и голяма част от тях е подложена на изпаряване. В изследваната област, водоносната система се възстановява от напояване и навлизане на морска вода, което влияе върху химичния състав на водата. Изследванията показват, че подпочвената вода в равнината Хебей е значително замърсена с нитратен азот. Чрез измерване на характеристиките на стабилните изотопи на азота и кислорода са определени източниците на замърсяване с азот за периода от 2009 до 2015 г. Средните концентрациите на нитратния азот са между 0.00 и 121.50 mg·L^{-1}, средната стойност за 7-годишния период е 17.64±1.55 mg·L^{-1}. Концентрациите на нитратен азот в различните райони са различни. Най-висока стойност на нитратен азот, 29.49 mg·L^{-1}, е установена в крайбрежния район, която надвишава 2.95 пъти стандарта за качество на питейната вода в Китай, следвана от стойността в предпланинския район, 15.78 mg·L^{-1}, надвишаваща стандарта 1.58 пъти. Най-ниска стойност е измерена в централния район, 3.88 mg·L^{-1}, която е под стандарта. Съгласно идентифицираните изотопи, в крайбрежния и централния район източниците на нитрати в подпочвените води са основно оборски тор и отпадъци, а в предпланинския район – земеделски торове.